

ChemComm

Chemical Communications

Accepted Manuscript

This article can be cited before page numbers have been issued, to do this please use: L. Zhong, Y. Bao, X. Yu and L. Feng, *Chem. Commun.*, 2019, DOI: 10.1039/C9CC04429A.



This is an Accepted Manuscript, which has been through the Royal Society of Chemistry peer review process and has been accepted for publication.

Accepted Manuscripts are published online shortly after acceptance, before technical editing, formatting and proof reading. Using this free service, authors can make their results available to the community, in citable form, before we publish the edited article. We will replace this Accepted Manuscript with the edited and formatted Advance Article as soon as it is available.

You can find more information about Accepted Manuscripts in the [Information for Authors](#).

Please note that technical editing may introduce minor changes to the text and/or graphics, which may alter content. The journal's standard [Terms & Conditions](#) and the [Ethical guidelines](#) still apply. In no event shall the Royal Society of Chemistry be held responsible for any errors or omissions in this Accepted Manuscript or any consequences arising from the use of any information it contains.

Journal Name

COMMUNICATION

Fe-doping into NiTe bulk crystal as a robust catalyst for electrochemical oxygen evolution reaction

Lei Zhong, Yufei Bao, Xu Yu and Ligang Feng*

cReceived 00th January 20xx,
Accepted 00th January 20xx

DOI: 10.1039/x0xx00000x

www.rsc.org/

Fe doping into NiTe bulk crystal was demonstrated as a robust catalyst for electrochemical oxygen evolution reaction. The promotion effect at least can be correlated to the significant electronic effect and the formation of lattice oxygen via bimetallic synergy by Fe doping.

Hydrogen fuel has been considered as a most promising resource in the upcoming era and hydrogen generated from water driven by sustainable energy like wind and solar energy is an alternative technique to remedy the intermittent nature of such new energy sources. Electrochemical water splitting is the key technique to realize the efficient energy transfer and oxygen evolution reaction (OER) is regarded as the bottleneck reaction for water splitting due to the complicated proton-coupled electron transfer process.^{1,2} Reliable non-precious electrocatalysts are highly desired to lower the cost of water-splitting devices because the state-of-the-art noble metal catalyst like RuO₂ and IrO₂ cannot meet the large scale demand from hydrogen production plants³⁻⁵.

Recently, Ni-based catalysts of sulfur group have been found active for OER because of the proper surface oxygen binding energy.⁶⁻⁸ Compared with O, S, Se atoms, Te atom has a more metallic character in nature that can increase the conductivity of catalyst system;^{9,10} alloy of Ni-Te is thus very promising to catalyze OER while it has not been intensively studied. A porous nickel telluride has been tentatively developed while it requires a very high overpotential of 679 mV to drive 10 mA cm⁻² for OER;¹¹ by increasing the conductivity, Ni foam or Ti mesh supported nanostructured NiTe can greatly enhance the catalytic ability with an overpotential of 315 mV to drive 10 mA cm⁻².¹² Fe in general can enhance the activity of Ni-based catalyst for OER through a Ni-Fe partial-charge-transfer activation process.¹³ The role of Fe is found to be significant, but not yet fully understood, in enhancing the activity of the Ni-

based catalyst for OER. A series of operando experiments and calculations demonstrated that Fe ion in Ni-Fe system would reduce the overpotential by altering the adsorption energy of OER intermediates, but the activity will be declined if the catalyst is rich of too many Fe due to the formation of low activity of FeOOH.^{1,14} While both high catalytic performance was found for the Ni-Fe system with more content of Fe in the form of Fe-Ni alloy or the trace amount of Fe with the form of surface doping. For example, the Ni-Fe alloy with a large amount of Fe in the system was very active for OER,¹⁵ meanwhile the Fe impurities (< 1 ppm) in the unpurified KOH electrolyte can also enhance the catalytic activity of some Ni-based catalyst.¹⁶

Driven by the above motivations, Fe-doping might be an efficient and cost-effective approach to boost NiTe catalyst for OER. To the best of our knowledge, however, no relevant report has been done before. Herein a Fe-doped NiTe nanoplate was developed for OER and the spectrum analysis showed a bulk crystal doping of Fe into NiTe that was different to previously reported Fe ion surface adsorption/doping. The electrochemical experiments demonstrated that Fe doped NiTe catalyst can greatly enhance the OER catalytic performance by a negative shift of 108 mV overpotential compared with NiTe alone to offer a benchmark current density of 10 mA cm⁻². Moreover, to our surprise, a trace amount of iron impurity in the electrolyte was not sufficiently found promoting the performance of NiTe for OER, while a highly stable catalytic activity was well observed for this Fe doped NiTe catalyst, namely without an initial activation process. However, without any doubt, the high performance should be attributed to Fe doping effect. The current work provides some novel understandings for the Fe-doping effect on Ni-based catalyst performance improvement.

The NiTe nanoplates doped by different contents of Fe (Fe-NiTe-1, 2 or 3) were synthesized by a one-step solvothermal approach (ESI). The pristine NiTe had a typical hexagonal crystal structure, and no other characteristic peaks assigned to metallic Fe or Fe oxide were found in all the Fe doped NiTe samples while the peak intensity of NiTe became stronger and the diffraction

^a School of Chemistry and Chemical Engineering, Yangzhou University, Yangzhou 225002, P.R. China. E-mail: ligang.feng@yzu.edu.cn, fenglg11@gmail.com

† Electronic Supplementary Information (ESI) available: See DOI: 10.1039/x0xx00000x

peaks shifted to the higher angle direction by increasing the amount of doped Fe (Fig. 1a-b). This phenomenon can be attributed to the distortion of lattice parameter of NiTe by the substitutions of smaller Fe for Ni. Fe-NiTe-2 had a layered nanoplate morphology (Fig. 1c and Fig. S1) and clear lattice fringes with d-spacing of 2.80 Å and 2.04 Å corresponding to (101) and (102) facet of NiTe were found, smaller than that of pristine NiTe⁹ because of the lattice distortion (Fig. 1d-e). A quasi-single crystal pattern was indicated by the ordered spots acquired from the selected area electron diffraction (SAED) pattern (Fig. 1f). The relevant elements of Ni, Fe, O and Te were also observed in the elemental mapping images (Fig. 1g-k) and the amount of Fe was measured to be 0.2%, 2.3% and 5.6 at.% for Fe-NiTe-1, 2 and 3 respectively by energy dispersive X-ray spectroscopy (EDS) (Fig. S2 and Table S1). The above results indicated the successful doping of Fe into NiTe bulk crystal through a simple solvothermal approach.

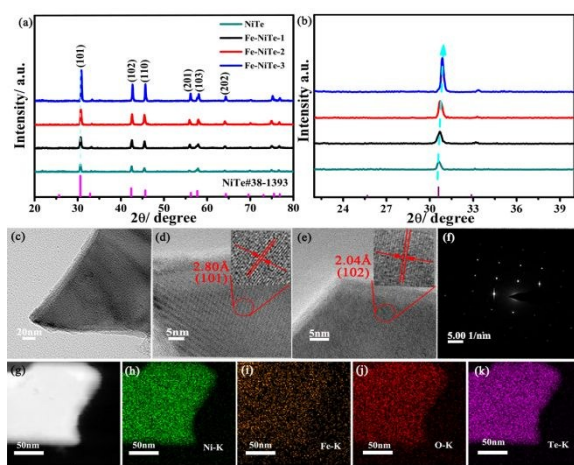


Fig. 1. XRD patterns (a) of pristine NiTe and Fe-doped NiTe catalysts; (b) the magnification of XRD patterns around 30°, (c-e) high-resolution TEM images, (f) corresponding SAED pattern, STEM mapping image (g) and corresponding elemental (h-k) distribution for Fe-NiTe-2 catalyst.

X-ray photoelectron spectroscopy (XPS) was carried out to probe the electronic structure and surface chemical configuration (Fig. S3a-b). Ni 2p spectrum had two bands of 2p_{3/2} and 2p_{1/2}, and each band can be deconvoluted into metallic Ni, divalent Ni and satellite peaks (Fig. 2a). The peak position of Ni 2p spectrum for Fe-NiTe-2 shifted to the high binding energy direction compared with pristine NiTe (Table S2). The high-resolution Te 3d spectrum had two components of 3d_{3/2} and 3d_{5/2}, and each component can be assigned to Te (0) and Te (+4) (Fig. 2b); compared with pristine NiTe catalyst, no obvious peak position shift was found on Te 3d spectrum but the content of Te(+4) for Fe-NiTe-2 was largely increased implying more TeO₂ was formed after Fe-doping (Table S3). Spin-orbit peaks of Fe 2p_{1/2} and Fe 2p_{3/2} were observed and they can be deconvoluted into Fe²⁺ and Fe³⁺ accompanying their satellite peaks (Fig. 2c). The deconvoluted O 1s peaks had four peaks at 529.5, 530.5, 531.7, and 533.2 eV, that can be assigned to metal-oxygen, lattice oxygen, the surface oxygen and oxygen species from the adsorbed water on the surface (Fig. 2d and Table S4).^{17,18} The content of the lattice-oxygen for Fe-NiTe-2

was significantly increased compared with the pristine NiTe because of the electronic structure change,¹⁹ the increased lattice-oxygen might be attributed to the lattice distortion arising from the Fe-doping effect that can release partial O atoms.²⁰ Lattice oxygen can participate in OER reaction and facilitate the reaction by reversible formation of surface vacancies and the increased metal-oxygen co-valence was considered critical in promoting the kinetics,¹⁵ thus a greatly increased catalytic performance for OER was observed (vide infra).

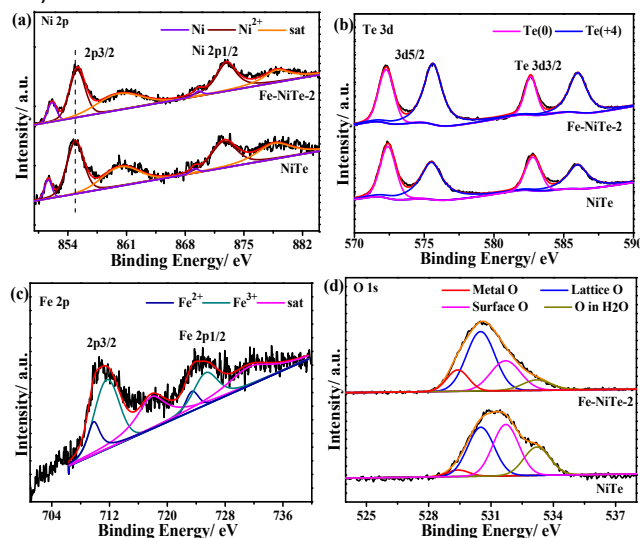


Fig. 2 XPS spectra of Ni 2p (a) and Te 3d (b) of NiTe and Fe-NiTe-2; Fe 2p (c) of Fe-NiTe-2, O 1s (d) of NiTe and Fe-NiTe-2.

The OER performance of Fe-NiTe nanoplates was evaluated by polarization curves compared with IrO₂ and pristine NiTe at 5 mV s⁻¹ (Fig. 3a). The pristine NiTe had the lowest catalytic performance requiring 388 mV overpotential to drive 10 mA cm⁻², that was consistent with the reports elsewhere.¹¹ After doping by Fe, the catalytic performance was significantly improved and the best performance was found on Fe-NiTe-2 that offered the benchmark current density with the overpotential of 280 mV, about 108 mV less than that of the pristine NiTe. This performance was also higher than other similar advanced catalyst materials and superior to the commercial IrO₂ catalyst requiring 330 mV overpotential to drive 10 mA cm⁻² (Table S5).

The kinetics information was probed by Tafel slope (Fig. 3b). The pristine NiTe had a slope value of 117 mV dec⁻¹ indicating the rate-determining step (RDS) of the formation of reactive –OH adsorbed on the metal surface;^{21,22} while the slope value was largely reduced by doping Fe into NiTe, and Fe-NiTe-2 had the smallest Tafel slope value of 40 mV dec⁻¹ following the RDS of the reactive –O formation and subsequent release as O₂.²³ The smaller Tafel slope implied more favorable OER kinetics. Nyquist plots from electrochemical impedance spectroscopy (EIS) were compared for all the concerned catalyst (Fig. 3c), the smallest R_{ct} value was obtained on the NiTe-Fe-2 elucidating the fast charge transfer and superior electro-catalytic behaviour after fitting the data by an equivalent circuit (Fig. S4 and Table S6). The increased charge transfer rate generally can be

attributed to the improved conductivity and surface adsorption ability.¹⁶ Compared with the pristine NiTe, Fe doping into NiTe bulk crystal not only increased the charge transfer rate but also changed the RDS during the catalyst process.

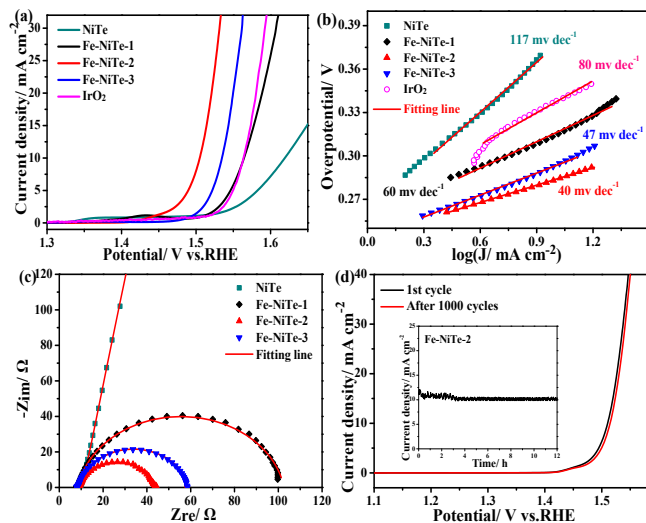


Fig. 3 Polarization curves with IR correction (a) and Tafel plots (b) of NiTe, Fe-doped NiTe and IrO₂. Nyquist plots (c) of NiTe, Fe-doped NiTe at 1.52 V vs. RHE. Polarization curves (d) of Fe-NiTe-2 before and after 1000 cycles (inset for chronoamperometry curve at 1.52 V vs. RHE).

Though only a minor amount of Fe was introduced into the NiTe system, the electrochemically active surface area was found evidently increased (Fig. S5 and Table S7a). The catalytic efficiency of the active sites was further evaluated by the specific activity and TOF (turnover of frequency) values²⁴, and NiTe-Fe-2 also exhibited the best catalytic efficiency (Fig. S6 and Table S7b). Specifically, the specific activity and TOF values at 300 mV overpotential were increased by 13 and 34 times compared with the pristine NiTe catalyst. The stability was compared by chronoamperometry (CA) and cyclic voltammetry (CV) technique. After 1000 CV cycling measurements, no obvious change was observed by comparing the initial and final polarization curves; consistently, CA measurement also demonstrated no obvious performance decay for 12 h to offer 10 mA cm⁻² signifying excellent electrocatalytic stability (Fig. 3d and its inset). The current efficiency was evaluated by comparing the amount of oxygen generated theoretically and experimentally at a constant voltage of 1.52 V vs. RHE for 1 h, the faradic efficiency nearly 100% was obtained for water oxidation (Fig. S7a). The electrolytes saturated by N₂ and O₂ were also compared for the OER performance study, and no obvious performance difference was found as shown in Fig. S7b.

The structure and surface state of Fe-NiTe-2 after OER test were studied to understand the catalytic process. Hexagonal crystal structure of Fe-NiTe-2 was maintained after the stability test, while interestingly the intensity of several peaks was found changed (Fig. 4a). Specifically, the intensity of diffraction peak for (102):(110) was increased from 1.27 to 1.74, and the intensity of (201):(103) peaks was reduced from 0.91 to 0.29 probably due to the surface oxidation. Considering the highly

stable catalytic performance, these facets of (110) and (201) might contribute little to maintain the high catalytic performance. Ni and Te elements were clearly indicated in the XPS spectrum for Fe-NiTe-2 catalyst after OER test. Due to the surface oxidation at high overpotentials for OER, the metallic state of Ni and Te was weakened while the content of high valence state was largely increased (Fig. S8a-d and Table S8-9). To our surprise, the profile of O1s of Fe-NiTe after OER test became more narrow and the peak position of the main peak was shifted to the low binding energy direction with more content of lattice oxygen formation. The well-kept high content of lattice oxygen in the catalyst system indicates its important role for the OER process (Fig. 4b, Table S10).

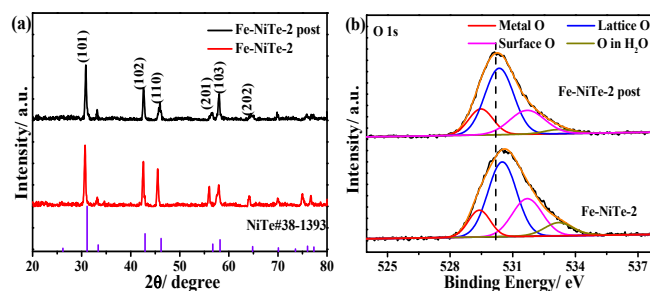


Fig. 4 XRD patterns (a) of Fe-NiTe-2 before and after OER electrolysis, XPS spectrum of O 1s (b) of Fe-NiTe-2 before and after OER electrolysis.

No obvious peak of Fe 2p was observed in the XPS spectrum indicating the dissolution of Fe during the catalytic process (Fig. S8e) while the presence of Fe can still be detected by the bulk EDS analysis (Fig. S9 and Table S11). Some reports observed the Fe impurity in the electrolyte can enhance the catalytic performance on some Ni-based catalyst for OER, while some work did not. The effect of the dissolved Fe in the electrolyte was also studied by comparing the fresh electrodes in the newly prepared electrolyte and Fe-containing electrolyte. For the pristine NiTe catalyst, the reduced catalytic performance was found both in the fresh electrolyte and Fe-containing electrolyte by increasing the cycling numbers and the current density was gradually reduced to reach a stable state after ca. 10 cycles (Fig. S10a-b and the inset); it means there was no sufficient promotion effect found on NiTe electrode from Fe impurities. While a very stable catalytic activity was found in the initial several cycles cycling process for Fe-NiTe-2 catalyst in the fresh electrolyte indicating no activation process required (Fig. 5a and the inset). Moreover, this stability can be well maintained for quite a long time as shown in the above dynamic and steady-state evaluation (Fig. 3d). During the long-term test, the Fe was found lost into the electrolyte and no Fe was detected in the catalyst surface, thus the Fe probably didn't contribute more to maintain the high catalytic performance. In order to exclude the effect of Fe impurity in the electrolyte, this aged electrode (after water cleaning) was moved to a fresh electrolyte and similar cases were found to the fresh Fe-NiTe-2 electrode in the fresh electrolyte that a quite stable catalytic performance was found (Fig. 5b). For this aged electrode, no Fe was found on the surface by XPS analysis, thus, basically the promotion from Fe adsorption was not supported or the trace

amount of Fe did not affect its catalytic performance. Similar cases have been recently found on Ni/Co catalyst.²⁵

Bimetallic NiFeOx had much better OER catalytic performance than FeOx and NiOx alone because of the synergetic effect between the two metals²⁶. Fe-doping can synergetic with Ni to decrease the adsorption free energies of intermediates on the catalysts surface, enhance the conductivity of the catalyst, induce partial charge transfer to activate the Ni centers for OER^{1,16}. Considering the above results, the performance improvement obviously can be attributed to the Fe-doping effect induced bimetallic synergy as confirmed by the structure and electronic state change after Fe doping. Once this doping structure was formed, the promotion effect was formed. It can also explain the promotion effect of Fe-NiTe-2 compared with pristine NiTe that no activation process was found in the initial cycles. It was proposed recently that lattice oxygen can adsorb OH⁻ to form -OO and surface O vacancy, the adsorbed OO evolves back to -OH with the generation of O₂(g).²⁷ The catalytic mechanism can be found in the supporting information (Figure S10c). From the XPS analysis, the Fe-doped into NiTe would initiate and maintain the high amount of lattice oxygen formation by lattice distortion, correspondingly high catalytic activity and stability performance for OER was observed even the Fe was gradually lost during the long-term stability test. The formation of the lattice oxygen in the system induced by electronic effect from Fe-doped into the crystal structure of NiTe would thus be a key factor to maintain the high catalytic activity and stability.

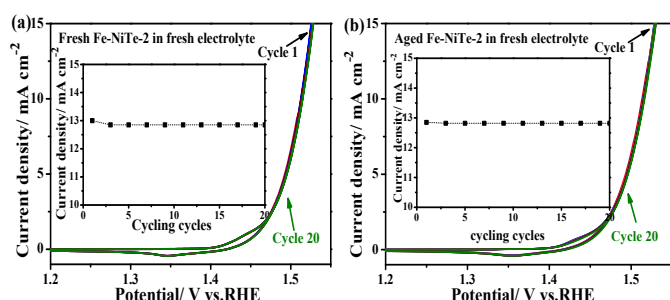


Fig. 5 Polarization curves without IR correction of fresh Fe-NiTe-2 (a) and aged Fe-NiTe-2 electrode, (b) in the fresh electrolyte. (inset for the current density at 1.52 V ($\eta=290$ mV) vs. Cycle numbers) Condition: Scan rate 5 mV s⁻¹, electrolyte: 1M KOH solution.

In summary, Fe doped into bulk crystal NiTe was demonstrated very active and stable for electrochemical oxygen evolution reaction. The current work found that the promotion effect at least can be correlated to the formation of a high amount of lattice oxygen in the Fe-doped NiTe catalyst system. The best catalytic performance of Fe-NiTe nanoplates can drive 10 mA cm⁻² with a low overpotential of 280 mV, about 108 mV less than the pristine NiTe catalyst. The impurity of Fe in the electrolyte was not found to affect the catalytic performance of NiTe, while Fe-doped into the crystal structure of NiTe caused a significant electronic effect via the Fe-Ni synergistic effect that greatly promoted the catalytic activity and stability for OER. The current findings contribute some novel understandings in the promotion effect of Fe for OER and

well support the significant role of lattice oxygen in the OER catalytic process.

DOI: 10.1039/C9CC04429A

The work is supported by the National Natural Science Foundation of China (21603041), A Project Funded by the Priority Academic Program Development of Jiangsu Higher Education Institution.

Conflicts of interest

There are no conflicts to declare.

References

- B. Xu, Z. Chen, X. Yang, X. Wang, Y. Huang and C. Li, *Chem. Commun.*, 2018, **54**, 9075-9078.
- X. Yang, Z. Zhao, X. Yu and L. Feng, *Chem. Commun.*, 2019, **55**, 1490-1493.
- I. S. Amiinu, X. Liu, Z. Pu, W. Li, Q. Li, J. Zhang, H. Tang, H. Zhang and S. Mu, *Adv. Funct. Mater.*, 2018, **28**, 1704638.
- Z. Liu, X. Yu, H. Xue and L. Feng, *J. Mater. Chem. A*, 2019, **7**, 13242-13248.
- Y. Xue, Y. Wang, H. Liu, X. Yu, H. Xue and L. Feng, *Chem. Commun.*, 2018, **54**, 6204-6207.
- L.-A. Stern, L. Feng, F. Song and X. Hu, *Energy Environ. Sci.*, 2015, **8**, 2347-2351.
- Z. Liu, H. Yu, B. Dong, X. Yu and L. Feng, *Nanoscale*, 2018, **10**, 16911-16918.
- S. Anantharaj, S. R. Ede, K. Sakthikumar, K. Karthick, S. Mishra and S. Kundu, *ACS Catal.*, 2016, **6**, 8069-8097.
- Z. Wang and L. Zhang, *Electrochem. Commun.*, 2018, **88**, 29-33.
- S. Anantharaj, K. Karthick and S. Kundu, *Inorg. chem.*, 2018, **57**, 3082-3096.
- K. S. Bhat, H. C. Barshilia and H. S. Nagaraja, *Int. J. Hydrogen Energy*, 2017, **42**, 24645-24655.
- Z. C. Wang and L. X. Zhang, *Chemelectrochem*, 2018, **5**, 1153-1158.
- M. S. Burke, M. G. Kast, L. Trotochaud, A. M. Smith and S. W. Boettcher, *J. Am. Chem. Soc.*, 2015, **137**, 3638-3648.
- D. Friebel, M. W. Louie, M. Bajdich, K. E. Sanwald, Y. Cai, A. M. Wise, M.-J. Cheng, D. Sokaras, T.-C. Weng, R. Alonso-Mori, R. C. Davis, J. R. Bargar, J. K. Nørskov, A. Nilsson and A. T. Bell, *J. Am. Chem. Soc.*, 2015, **137**, 1305-1313.
- Z. Liu, X. Yu, H. Yu, H. Xue and L. Feng, *ChemSusChem*, 2018, **11**, 2703-2709.
- L. Trotochaud, S. L. Young, J. K. Ranney and S. W. Boettcher, *J. Am. Chem. Soc.*, 2014, **136**, 6744-6753.
- L. Yang, L. Chen, D. Yang, X. Yu, H. Xue and L. Feng, *J. Power Sources*, 2018, **392**, 23-32.
- L. Yang, B. Zhang, B. Fang and L. Feng, *Chem. Commun.*, 2018, **54**, 13151-13154.
- T. Zhou, Z. Cao, P. Zhang, H. Ma, Z. Gao, H. Wang, Y. Lu, J. He and Y. Zhao, *Sci. Rep.*, 2017, **7**, 46154.
- S. Yu, H. J. Yun, D. M. Lee and J. Yi, *J. Mater. Chem.*, 2012, **22**, 12629-12635.
- Y.-H. Fang and Z.-P. Liu, *ACS Catal.*, 2014, **4**, 4364-4376.
- S. Anantharaj, S. R. Ede, K. Karthick, S. Sam Sankar, K. Sangeetha, P. E. Karthik and S. Kundu, *Energy Environ. Sci.*, 2018, **11**, 744-771.
- Y. Tong, X. Yu and G. Shi, *Phys. Chem. Chem. Phys.*, 2017, **19**, 4821-4826.
- S. Anantharaj and S. Kundu, *ACS Energy Letters*, 2019, **4**, 1260-1264.
- Y. Li, L. Hu, W. Zheng, X. Peng, M. Liu, P. K. Chu and L. Y. S. Lee, *Nano Energy*, 2018, **52**, 360-368.
- D. A. Corrigan, *J. Electrochem. Soc.*, 1987, **134**, 377-384.

Journal Name

COMMUNICATION

27 X. Rong, J. Parolin and A. M. Kolpak, *ACS Catal.*, 2016, **6**, 1153-1158.

View Article Online
DOI: 10.1039/C9CC04429A